CHAPTER V

Tuning the Erosion Rate of Artificial Protein Hydrogels through Control of Network Topology

Abstract

Erosion behaviour governs the use of physical hydrogels in biomedical applications ranging from controlled release to cell encapsulation. Genetically engineered protein hydrogels offer unique means of controlling the erosion rate by engineering their amino acid sequences and network topology. Here, we show that the erosion rate of such materials can be tuned by harnessing selective molecular recognition, discrete aggregation number and orientational discrimination of coiled-coil protein domains. Hydrogels formed from a triblock artificial protein bearing dissimilar helical coiled-coil end domains (P and A) erode more than one hundredfold slower than hydrogels formed from those bearing the same end domains (either P or A). The reduced erosion rate is a consequence of the fact that looped chains are suppressed because P and A tend not to associate with each other. Thus, the erosion rate can be tuned over several orders of magnitude in artificial protein hydrogels, opening the door to diverse biomedical applications.

5.1 Introduction

Artificial protein hydrogels assembled through aggregation of leucine zipper domains have the capacity for self-assembly encoded in the protein sequence[1]. Gelation does not require chemical crosslinking reagents that can compromise material safety in biomedical applications. The modular nature and fidelity of the biosynthetic method used to create these artificial proteins allow different biological determinants—including cell binding domains and enzyme recognition sites—to be incorporated readily in precisely controlled fashion. These advantages make genetically engineered, physically crosslinked hydrogels promising candidates for applications in biomedical fields such as controlled release and tissue engineering.

Control of erosion rate is a critical design objective for biomedical hydrogels[2-6]. For chemically crosslinked hydrogels, erosion behavior is controlled by introducing linkages susceptible to hydrolysis[6] or enzymatic cleavage[5]. On the other hand, many physical hydrogels exhibit undesirably rapid erosion when placed in open aqueous environments[2,7-12]. For hydrogels assembled from hydrophobically modified ethylene oxide polymers (PEOs), this issue has been addressed by controlling phase separation behavior[13-15]; molecular structure is adjusted to produce a transient network that coexists with a dilute sol phase in order to confer slow surface erosion. For ionically crosslinked alginate hydrogels, covalent cross-linking has been used to improve hydrogel stability[2]. Other examples of rapidly-eroding physical hydrogels include those formed by PEO-PPO-PEO block copolymers[11] and by mixtures of PEOs and

α-cyclodextrin[10]. For the physically crosslinked leucine zipper hydrogels reported to date (e.g. $AC_{10}A$, Fig. 5.1), rapid erosion was observed in open solutions. For example, a 1-mm-thick $AC_{10}A$ hydrogel (7% w/v) dissolves completely within 2.9 hours in 100 mM, pH 7.6 phosphate buffer. Such rapid dissolution precludes applications in which the gel must persist while immersed in excess fluid.

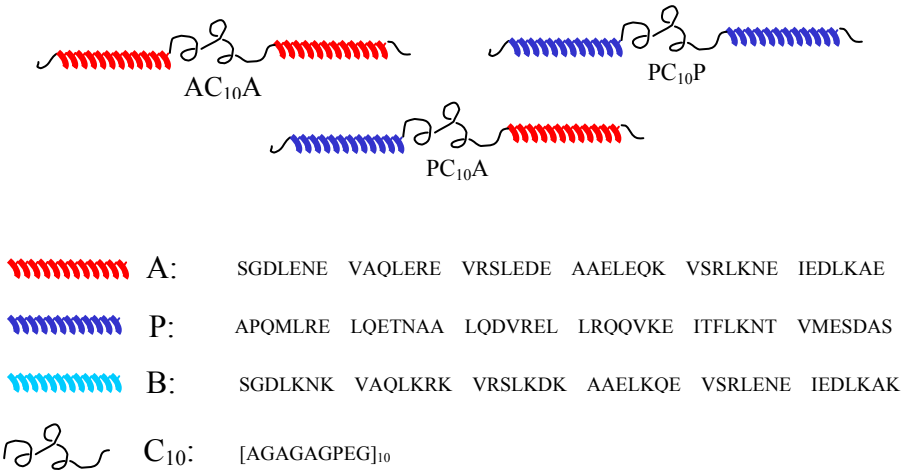

Figure 5.1 Schematic representations of triblock proteins and the amino acid sequences of major domains. The major domains of each triblock protein are joined by short sequences of amino acids introduced in the construction of the cloning and expression vectors. Each protein carries an N-terminal hexahistidine tag to allow the protein to be purified by affinity chromatography on a nickel nitrilotriacetic acid.

Our previous studies of the structural and dynamic properties of $AC_{10}A$ hydrogels in closed systems revealed that these multi-domain protein chains have a strong tendency to form intramolecular loops[16]. The aggregation number of the associative

domain (A) is small (4)[16,17], and association is transient[16]. These three factors all contribute to the fast erosion of $AC_{10}A$ networks. Disengaged clusters form readily because intramolecular loops are favored and the aggregation number of the leucine zipper domain is small (Fig. 5.2a). Since the strand exchange time of the leucine zipper domain is on the order of 100 to 1000 seconds[16] near physiological pH, the

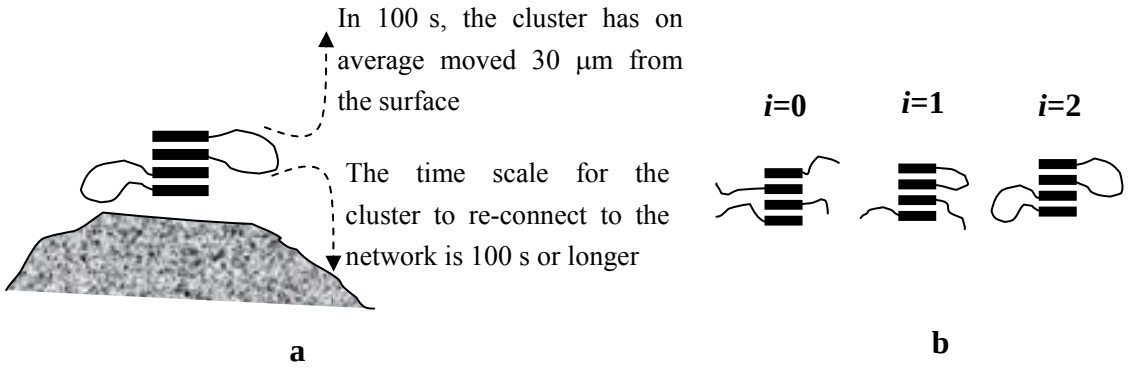

Figure 5.2 Structural and dynamic properties underlying the fast erosion of $AC_{10}A$ hydrogels. a, Disengaged clusters form readily in the system because of the strong tendency toward intramolecular association and the small aggregation number of the associative domain. They are lost from the surface through diffusion before re-connecting to the network. b, Three possible states of tetrameric aggregates designated by the number of loops *i*.

time scale for disengaged clusters to re-bind to the network is 100 seconds or longer. In 100 seconds, a cluster with diffusivity of 10^{-7} cm^2/s has on average moved 30 μm away from the surface of the network, and is lost to the surrounding buffer before it

can re-connect to the network. The transient nature of the association continuously releases disengaged clusters, leading to a quasi-steady concentration of free clusters at the surface such that their diffusive flux balances their rate of creation at the network surface. Consequently, the network erodes at a constant rate from its surface. The rate of cluster release is governed by the probability of a cluster simultaneously losing all of its connections to the network. We infer that among the structural and dynamic properties that cause the fast erosion of $AC_{10}A$ networks, an essential factor is facile intramolecular association. At any given moment, many tetrameric aggregates of the A domain have no connection to the network (Fig. 5.2b i=2), and many adopt configurations in which exchange of a single leucine zipper can liberate the cluster (Fig. 5.2b i=1).

We speculated that suppressing intramolecular loops in the networks would substantially reduce the erosion rate, and that intramolecular loops could be suppressed by engineering two dissimilar endblocks that do not associate with each other. Fidelity of molecular recognition between protein domains, which is the basis for many aspects of biological function, provides us the opportunity to control network structure and reduce the erosion rate. In particular, we speculated that the coiled-coil domain derived from the N-terminal fragment of rat cartilage oligomeric matrix protein (COMP)[18] would be likely to prefer homo-oligomerization (self-aggregation of identical protein domains) rather than hetero-oligomerization (aggregation of different protein domains) with leucine zipper A. The coiled-coil

domain from COMP assembles into five-stranded bundles[19,20]; in contrast, the A domain assembles into tetramers. The different packing structures of these two domains should suppress hetero-oligomerization.

5.2 Results and discussion

This expectation was confirmed experimentally. To create the coiled-coil domain (designated P) for physical association in a reversible gel, the amino acid sequence of the wild-type COMP domain was modified slightly to avoid chemical crosslinking: the two cysteine residues were mutated into serine residues. A DNA fragment encoding the P domain was inserted into pQE9 and expressed in *Escherichia coli*. The resulting protein was expressed, and its expected molar mass (6942 Da) was confirmed by mass spectral analysis. Multi-angle light scattering measurements for 30 μM and 107 μM P solutions revealed average molecular weights of 34310±380 and 35260±160, respectively, suggesting that the cysteine-free variant retains pentameric association. Native electrophoresis of a solution containing AC_{10} and P (100 μM in each protein, incubated at pH 7.6 and room temperature overnight) yielded two separate bands in which proteins migrated at the same rates as AC_{10}–aggregates and P-aggregates, respectively (Fig. 5.3a). As a control experiment in which hetero-oligomerization is dominant, retardation in migration of AC_{10} due to its strong association with leucine zipper B[21] (sequence shown in Fig. 5.1) was observed on the same gel. The results of these experiments suggest that the A and P domains

discriminate against each other in mixtures. Mass spectral analysis of the trypsin digests of the resolved protein bands provided further confirmation that each band contains only one species: each band yielded signals corresponding either solely to P or solely to AC_{10} (Fig. 5.3b).

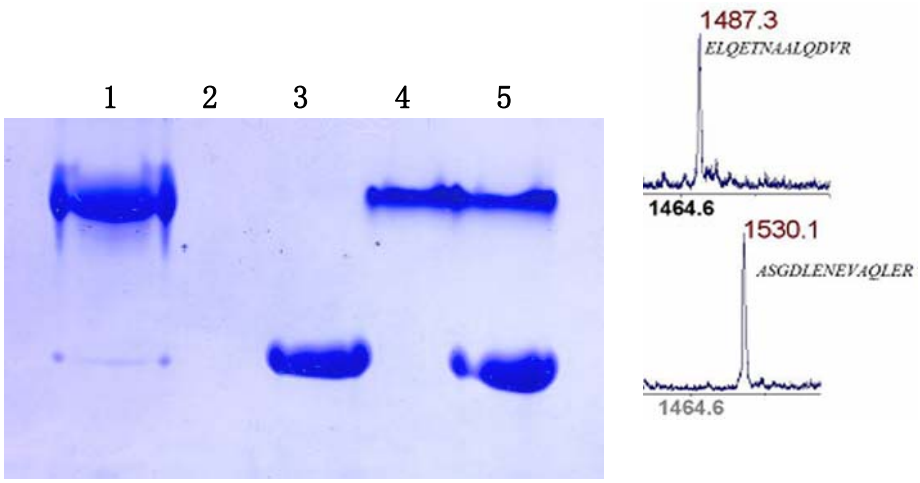

Figure 5.3 Coiled-coil domains A and P do not associate with each other. a, Native electrophoresis of recombinant proteins. Lane 1. AC_{10} + B; 2. B; 3. AC_{10}; 4. P; 5. AC_{10} + P. Protein B by itself does not migrate into the gel due to its net positive charge. b, Mass spectral analysis of trypsin digests of the proteins in the two bands excised from lane 5. ELQETNAALQDVR and ASGDLENEVAQLER are fragments from P and AC_{10}, respectively.

New triblock proteins $PC_{10}A$ and $PC_{10}P$ (Fig. 5.1) were then expressed and characterized. The molar masses of $PC_{10}A$, $PC_{10}P$ and $AC_{10}A$ are 20860 Da, 20486

Da and 22105 Da, respectively. All three proteins have nearly identical midblocks and their coiled-coil domains are the same length (six heptad repeats). They all assemble into hydrogels in aqueous solutions. Rheological oscillatory shear measurements

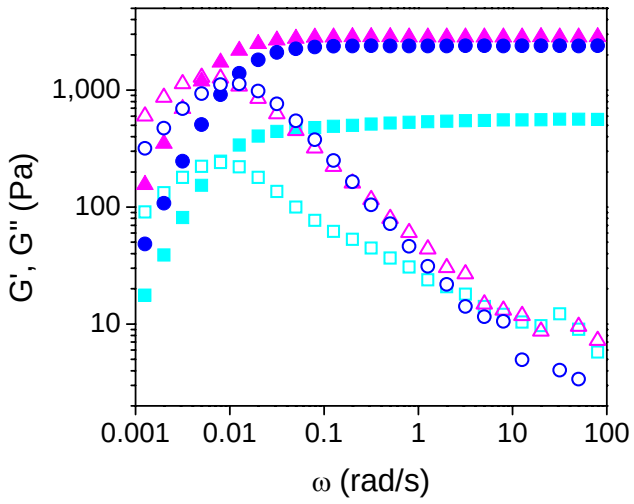

Figure 5.4 Dynamic moduli (closed symbols for storage moduli; open symbols for loss moduli) of $AC_{10}A$ (■, □); $PC_{10}P$ (●, ○); and $PC_{10}A$ (▲, △) hydrogels. (7% w/v, 100 mM phosphate buffer, pH 7.6, 22 °C)

revealed increased rigidity of the new materials compared to $AC_{10}A$ hydrogels (Fig. 5.4). The normalized plateau storage moduli G'_{∞}/nkT (G'_{∞}, plateau storage modulus; n, chain number density) were 0.35±0.01, 0.29±0.02 and 0.07±0.00 for $PC_{10}A$, $PC_{10}P$ and $AC_{10}A$, respectively, suggesting that loops are suppressed in the new materials.

Suppression of looped chains in $PC_{10}A$ gels was expected because the A domain and the P domain do not associate with each other. A decrease in the fraction

of looped chains in $PC_{10}P$ gels relative to $AC_{10}A$ might result from two structural features of the associative domains. First, the odd aggregation number of the pentameric P domain limits the maximum loop fraction in $PC_{10}P$ networks to 80%, while there is no such constraint for $AC_{10}A$ networks with tetrameric junctions. Another possible source of this different behavior may be the orientation of the A and P peptide strands in their aggregates. The isolated COMP pentamerization domain forms exclusively parallel aggregates[18,22], while our previous studies have shown that the isolated A domain can adopt an antiparallel orientation[16]. The length of the helical domains (A or P) with six heptad repeats is 65 Å[23], while the average hydrodynamic diameter of midblock chains is 40 Å as determined by quasi-elastic light scattering measurements[16]. Therefore, the midblock would have to stretch for a loop to form with parallel association of the end domains. Loops form readily in $AC_{10}A$ networks because A can adopt antiparallel association. In contrast, formation of loops in $PC_{10}P$ networks costs energy either to stretch the midblock (if the endgroups are parallel) or to adopt a thermodynamically unfavorable orientation (if the endgroups are antiparallel).

Network relaxation dynamics of $PC_{10}A$, $PC_{10}P$, and $AC_{10}A$ hydrogels are revealed from the frequencies of the maxima in their loss moduli (Fig. 5.4). The dominant stress relaxation time (the reciprocal of the frequency at which the loss modulus peaks) of the $PC_{10}P$ gel (ca. 80 s) is shorter than those of the $AC_{10}A$ gel (ca. 130 s) and $PC_{10}A$ gel (ca. 200 s). Our previous studies showed that the dominant

stress relaxation time of an $AC_{10}A$ hydrogel is strongly correlated with the strand exchange time of the leucine zipper domain[16], but systematically shorter than the strand exchange time by a factor of 3~4 due to the formation of looped chains[16,24]. The higher storage modulus of the $PC_{10}P$ gel relative to the $AC_{10}A$ gel suggests fewer loops and therefore a closer correspondence of the stress relaxation and strand exchange times. Therefore, the rate of exchange of the P domain must be greater than that of the A domain to account for the faster relaxation of $PC_{10}P$ relative to $AC_{10}A$.

Despite the fact that P domains undergo more rapid strand exchange, introduction of P into multi-domain proteins results in materials characterized by slower erosion rates in open aqueous solutions. The erosion profiles of 7% w/v $AC_{10}A$, $PC_{10}P$, and

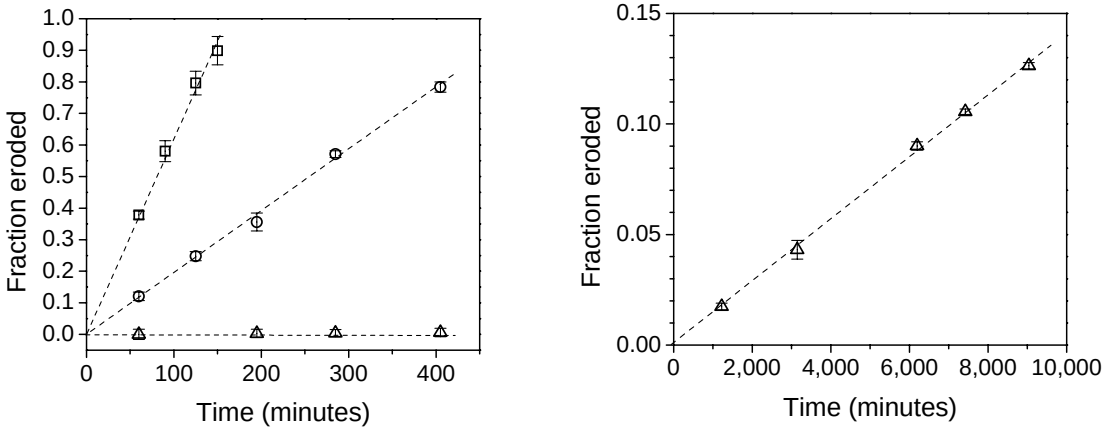

Figure 5.5 Erosion profiles of $AC_{10}A$ (□); $PC_{10}P$ (○); and $PC_{10}A$ (△) hydrogels. (7% w/v, 100 mM phosphate buffer, pH 7.6, room temperature) The surface area of each gel is 0.5672 cm^2. The total mass of each gel is 60 mg. Erosion rates: 4.3×10^{-2} mg/cm^2min for $AC_{10}A$, 1.3×10^{-2} mg/cm^2min for $PC_{10}P$ and 9.6×10^{-5} mg/cm^2min for $PC_{10}A$.

$PC_{10}A$ hydrogels (Fig. 5.5) all show linear mass-loss vs. time profiles, indicating that erosion is occurring at the surface rather than in the bulk. The erosion rates are 4.3×10^{-2} mg/cm^{2}min, 1.3×10^{-2} mg/cm^{2}min, and 9.6×10^{-5} mg/cm^{2}min for $AC_{10}A$, $PC_{10}P$, and $PC_{10}A$ hydrogels, respectively. A $PC_{10}A$ gel erodes ca. 500 times more slowly than an $AC_{10}A$ gel, and ca. 135 times more slowly than a $PC_{10}P$ gel. For 1-mm-thick samples, an $AC_{10}A$ gel dissolves completely within 2.9 hrs, while a $PC_{10}A$ gel erodes in 50 days.

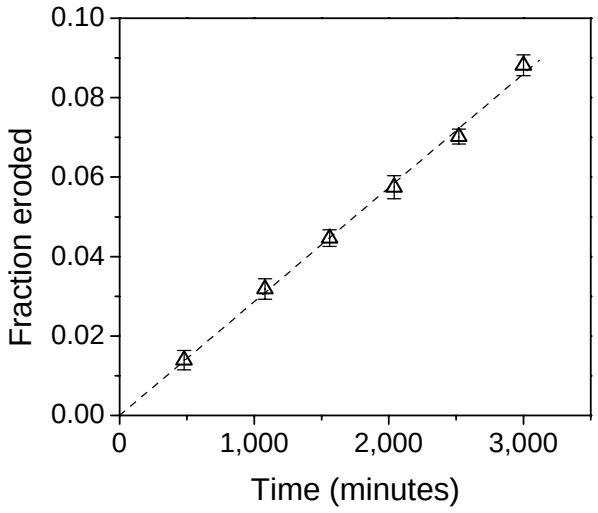

Figure 5.6 The erosion profile of $PC_{10}A$ hydrogels (7% w/v) at 37 °C in Dulbecco's Phosphate Buffered Saline (1x, pH 7.4). The surface area of each gel is 0.5672 cm^2. The total mass of each gel is 60 mg. The erosion rate is 1.9×10^{-4} mg/cm^{2}min.

The gradual erosion of $PC_{10}A$ at 22 °C into 100 mM phosphate buffer also holds for erosion under physiologically relevant conditions. The erosion rate of 7% w/v $PC_{10}A$ gels at 37 °C in Dulbecco's Phosphate Buffered Saline (PBS) (1x, pH 7.4) is 1.9×10^{-4} mg/cm^{2}min, only two-fold greater than that at room temperature(Fig. 5.6).

The erosion of $PC_{10}A$ at 37 °C is still more than 200 times slower than that of $AC_{10}A$ at room temperature (a 1-mm-thick sample erodes in 25 days). Erosion of $PC_{10}A$ at 37 °C in Dulbecco's Modified Eagle's Medium (DMEM) with 10% fetal bovine serum added was monitored by gel electrophoresis of the supernatant followed by densitometry analysis of the $PC_{10}A$ protein bands using NIH ImageJ. The erosion rate is consistent with that in PBS (Fig. 5.7).

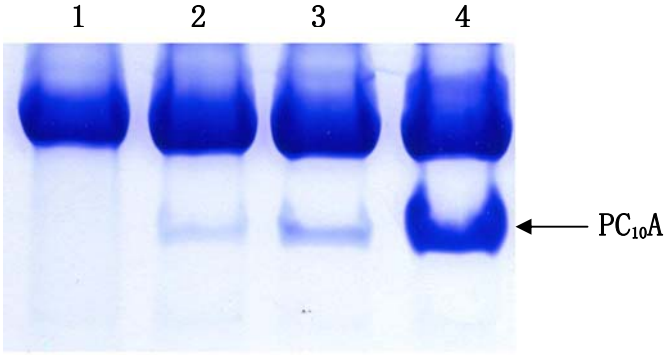

Figure 5.7 The erosion of $PC_{10}A$ hydrogels at 37 °C in 3 ml of Dulbecco's Modified Eagle's Medium (DMEM) with 10% fetal bovine serum added monitored over 4 days.Lane 1. medium; 2. supernatant collected after the gel eroded for 48 hrs; 3. supernatant collected after the gel eroded for 96 hrs; 4. $PC_{10}A$ solution at a concentration corresponding to 100% dissolved gel in the medium.

The erosion rate of $PC_{10}A$ networks is reduced by 2~3 orders of magnitude relative to $AC_{10}A$ and $PC_{10}P$ networks. Since $PC_{10}A$ is constituted from the same associative domains as $AC_{10}A$ and $PC_{10}P$, the significant decrease in erosion rate cannot originate from the strand exchange kinetics of the associative domains. The

slow erosion of $PC_{10}A$ networks is not a consequence of phase separation behavior either—a constant erosion rate for $PC_{10}A$ gels was observed over a period of 7 days (Fig. 5.5b) even though the supernatant was not refreshed, indicating that the surrounding solution was far from saturation. It is control of network topology that causes the slow erosion of $PC_{10}A$ networks. Among the three gels, $PC_{10}A$ exhibits the highest G'_∞/nkT value, suggesting that it has the fewest intramolecular loops. The concomitant decrease in erosion rate supports the design concept proposed here: controlling network structure to suppress loops reduces erosion rates of transient networks formed from artificial proteins. The erosion rate decreases much more strongly than the modulus increases due to the different physics involved. Erosion requires that free species be present at the surface of the gel. In the extreme that loops are forbidden, the concentration of free species at the surface of the gel can be reduced by orders of magnitude. On the other hand, the upper bound on the modulus is nkT when all strands form bridges. The modulus lies between nkT and its minimum value at the percolation threshold. The range of the modulus is therefore constrained to vary by less than one order of magnitude.

The small, discrete number of endblocks per aggregate (m=4 for A and m=5 for P) is conducive to a simple statistical analysis of the relationship between the fraction of looped chains q and the number of effective crosslinks in the network. The model also gives qualitative insight into the effects of q on the erosion rate. Consider a solution of n chains having tetrameric aggregates of the endblocks. Each aggregate has three

possible states (Fig. 5.2b), with i=0, 1, or 2 loops, respectively. Of the $2n/m$ aggregates, the fraction of the aggregates having i loops (f_i) is related to the overall fraction of looped chains q through balances on the number of looped chains and the total number of aggregates (n/2):

$$\frac{2n}{m}(f_1 + 2f_2) = nq \qquad (1)$$

$$\sum_{i=1}^{3} f_i = 1 \qquad (2)$$

These equations hold for both tetrameric and pentameric aggregates. To solve for the f_i in terms of q, it is useful to define the relative probability that an aggregate has a single loop:

$$f_1 / f_0 \equiv s \qquad (3)$$

Since the relative probability that an aggregate has two loops is:

$$f_2 / f_0 = \frac{1}{2}s^2 \quad \text{(two loops in state } i\text{=2 are indistinguishable)} \qquad (4)$$

The conservation equations (1) and (2) yield a quadratic equation for s in terms of q. The solution is:

$$s = \frac{\frac{2}{m} - q - \sqrt{(\frac{2}{m} - q)^2 - 2q(q - \frac{4}{m})}}{q - \frac{4}{m}} \qquad (5)$$

In terms of s, the fraction of aggregates in each state is:

$$f_i = \frac{s^i}{i!} \cdot \frac{1}{\sum_{i=0}^{2} \frac{s^i}{i!}} \quad (i\text{=0, 1, 2}) \qquad (6)$$

An aggregate may form a network junction if it has three or more bridges. For

tetrameric aggregates, this includes only i=0 aggregates. So its modulus relative to a loop-free network (q=0) is simply:

$$\frac{G'_{\infty}}{G'_{\infty(q=0)}} = f_0 \qquad (m=4)$$

The fraction of tetrameric aggregates that are not connected to the network is:

$$\phi_{free} = f_2 \qquad (m=4)$$

If we use the observed modulus of a 7% w/v $PC_{10}A$ as a q = 0 value, then a 7% w/v $AC_{10}A$ gel has $f_0 \approx 0.2$, which can be explained in terms of loop fraction $q \approx 0.6$ (Table 1). For this value of q, 40% of the aggregates are free (f_2 = 0.4), consistent with the observation of rapid erosion.

In the case of $PC_{10}P$, which has pentameric aggregates of the endblocks, the normalized modulus reflects aggregates with i=0 and i=1 because both have ≥3 bridges: $\frac{G'_{\infty}}{G'_{\infty(q=0)}} = f_0 + f_1$. Again using the modulus of a $PC_{10}A$ gel as a q = 0 value, we infer that a 7% w/v $PC_{10}P$ gel has $f_0+f_1 \approx 0.8$, corresponding to $q \approx 0.3$. For this value of q, 20% of the aggregates are in the state i=2. However, these aggregates do not represent free species, since there is still a bridging chain. An upper bound on the erosion rate of $PC_{10}P$ is provided by considering a single attachment to be released so frequently that it does not limit the erosion rate. Then a $PC_{10}P$ gel would have an erosion rate that is half that of an $AC_{10}A$ gel ($f_{2(m=5)}/f_{2(m=4)} \approx 0.5$). The greater the effect of the attached arm, the slower $PC_{10}P$ would erode. The observed erosion rate of $PC_{10}P$ is 1/4~1/3 that of $AC_{10}A$—surprisingly close to the upper bound.

In contrast to $AC_{10}A$ and $PC_{10}P$, it is not possible for a single oligomer of endblocks to leave a $PC_{10}A$ gel due to the strong suppression of hetero-oligomerization. Instead, an A tetramer cannot be liberated without bringing four P domains with it. Compared to larger clusters, a pair of P and A aggregates ("P-A pair") with four bridges to each other is the most probable species that can be released, although liberation of such species is associated with some free energy penalty (for example, for a P tetramer relative to a P pentamer). The erosion rate of $PC_{10}A$ relative to that of $AC_{10}A$ reflects, in part, the small probability of free P-A pairs in $PC_{10}A$. If an aggregate has *m* coiled-coils in it and *t* neighboring aggregates, then the probability that it forms all of its *m* bridges with just one neighbor is t^{1-m}. For example, for a tetrameric aggregate having 6 neighbors, the probability of the occurrence of such species is ~1/200. In contrast, ca. 40% of the aggregates have two loops and are free in an $AC_{10}A$ gel. An additional reduction in erosion rate of $PC_{10}A$ is due to the energy penalty noted above. This analysis is consistent with the observation that a $PC_{10}A$ gel erodes 2~3 orders of magnitude more slowly than an $AC_{10}A$ gel.

Control of network topology substantially expands the range of material properties that can be achieved in artificial protein hydrogels. Previously established principles for engineering thermal and pH responsiveness of coiled-coil domains[25-30] can now be coupled with molecular design for desired network structure to confer properties that are otherwise inaccessible. Design principles based on network

topology proved effective under physiologically relevant conditions. Prior results demonstrated that these gels are non-toxic (by viability of mammalian 3T3 fibroblast cells cultured in the presence of $AC_{10}A$[16]). Thus, the approach presented here can be used to optimize systems for a broad range of applications in biology and medicine.

5.3 Materials and methods

The DNA segment encoding the P domain was created by PCR assembly. Expression vectors pQE9PC_{10}P, pQE9PC_{10}A, and pQE9P were constructed by standard recombinant DNA techniques. Proteins were expressed and purified as described previously[1]. To determine the oligomerization state of the P domain, multi-angle static light scattering measurements were carried out on a DAWN EOS light scattering instrument (Wyatt Technology Corporation, CA) and the data were analyzed with Debye plots by using a dn/dc value of 0.185[31]. To examine whether P and A domains tend to associate with each other, native electrophoresis was performed on 12% polyacrylamide gels using the standard protocol with SDS and reducing agents omitted from all solutions. The resolved protein bands were cut from the gel. After the Coomassie stain was removed from each protein band[32], digestion with 0.02 mg/mL trypsin (Promega) was allowed to proceed at 37 °C overnight. Mass spectral analysis of the trypsin digests was performed on an Applied Biosystems Voyager mass spectrometer using MALDI matrix α-cyano-β-hydroxycinnamic acid (10 mg/mL in 50% CH_3CN). Rheological oscillatory shear measurements for $PC_{10}A$,

$PC_{10}P$, and $AC_{10}A$ gels were carried out on an RFS III rheometer (TA Instruments, New Castle, Delaware) with a cone-and-plate geometry (0.04 rad cone angle and 25-mm diameter). To measure the erosion rates of hydrogels, 1-mm-thick flat gel films were made in cylindrical plastic containers of 8.5 mm diameter and 3 mm height, which were then placed in 3 mL phosphate buffer (100 mM, pH 7.6) in scintillation vials with the gel surfaces facing down. The erosion profiles were determined by measurement of the protein concentration in the supernatant at successive time points. Protein concentrations were determined by measuring the absorbance at 280 nm on a Cary 50 Bio UV-vis spectrophotometer (Varian, Palo Alto, CA). The experiments were performed in triplicate.

To characterize erosion of $PC_{10}A$ in the presence of serum proteins, erosion from one face of an 8.5 mm diameter × 1.06 mm thick gel sample at 37 °C into 3 ml of Dulbecco's Modified Eagle's Medium (DMEM) with 10% fetal bovine serum added was monitored over 4 days. To distinguish $PC_{10}A$ from the serum protein background, the medium was sampled, mixed with loading buffer and separated using SDS-polyacrylamide gel electrophoresis. The volume of medium sample loaded onto each lane was kept constant (10 μl). Protein bands were visualized by staining with Coomassie Blue. The gel was digitally imaged and densitometry analysis of $PC_{10}A$ bands was performed using NIH ImageJ. Interpretation of $PC_{10}A$ concentrations in medium was based on calibration $PC_{10}A$ solutions of known concentrations. Densitometry analysis indicates that at 48 hrs and 96 hrs 6% and 15%, respectively, of

the initial gel had dissolved. Although there is certain uncertainty in the present method, it shows that the erosion time in the presence of serum proteins is on the same order as the time for erosion in PBS.

Acknowledgment. The authors acknowledge the NSF Center for the Science and Engineering of Materials for financial support.

5.4 References

(1) Petka, W. A.; Harden, J. L.; McGrath, K. P.; Wirtz, D.; Tirrell, D. A. *Science* **1998**, *281*, 389.

(2) Lee, K. Y.; Mooney, D. J. *Chem. Rev.* **2001**, *101*, 1869.

(3) Anseth, K. S.; Metters, A. T.; Bryant, S. J.; Martens, P. J.; Elisseeff, J. H.; Bowman, C. N. *J. Control. Rel.* **2002**, *78*, 199.

(4) Yamaguchi, N.; Kiick, K. L. *Biomacromolecules* **2005**, *6*, 1921.

(5) Rizzi, S. C.; Hubbell, J. A. *Biomacromolecules* **2005**, *6*, 1226.

(6) Kim, B. S.; Hrkach, J. S.; Langer, R. *Journal of Polymer Science Part a-Polymer Chemistry* **2000**, *38*, 1277.

(7) Kaczmarski, J. P.; Glass, J. E. *Macromolecules* **1993**, *26*, 5149.

(8) Lundberg, D. J.; Brown, R. G.; Glass, J. E.; Eley, R. R. *Langmuir* **1994**, *10*, 3027.

(9) Tam, K. C.; Jenkins, R. D.; Winnik, M. A.; Bassett, D. R. *Macromolecules*

1998, *31*, 4149.

(10) Li, J.; Ni, X. P.; Leong, K. W. *Journal of Biomedical Materials Research Part A* **2003**, *65A*, 196.

(11) Anderson, B. C.; Pandit, N. K.; Mallapragada, S. K. *Journal of Controlled Release* **2001**, *70*, 157.

(12) Wang, C.; Stewart, R. J.; Kopecek, J. *Nature* **1999**, *397*, 417.

(13) Pham, Q. T.; Russel, W. B.; Thibeault, J. C.; Lau, W. *Macromolecules* **1999**, *32*, 2996.

(14) Tae, G.; Kornfield, J. A.; Hubbell, J. A.; Johannsmann, D.; Hogen-Esch, T. E. *Macromolecules* **2001**, *34*, 6409.

(15) Francois, J.; Beaudoin, E.; Borisov, O. *Langmuir* **2003**, *19*, 10011.

(16) Shen, W., Ph.D. Dissertation; California Institute of Technology, CA 2005.

(17) Kennedy, S. B. Ph.D. Dissertation, Ph.D. Dissertation; University of Massachusetts Amherst, MA 2001.

(18) Malashkevich, V. N.; Kammerer, R. A.; Efimov, V. P.; Schulthess, T.; Engel, J. *Science* **1996**, *274*, 761.

(19) Efimov, V. P.; Engel, J.; Malashkevich, V. N. *Proteins-Structure Function and Genetics* **1996**, *24*, 259.

(20) Efimov, V. P.; Lustig, A.; Engel, J. *Febs Letters* **1994**, *341*, 54.

(21) Petka, W. A., Ph.D. Dissertation; University of Massachusetts Amherst, MA 1997.

(22) Ozbek, S.; Engel, J.; Stetefeld, J. *Embo Journal* **2002**, *21*, 5960.

(23) Hodges, R. S. *Biochemistry and Cell Biology-Biochimie Et Biologie Cellulaire* **1996**, *74*, 133.

(24) Annable, T.; Buscall, R.; Ettelaie, R.; Whittlestone, D. *Journal of Rheology* **1993**, *37*, 695.

(25) Harbury, P. B.; Zhang, T.; Kim, P. S.; Alber, T. *Science* **1993**, *262*, 1401.

(26) Kohn, W. D.; Hodges, R. S. *Trends in Biotechnology* **1998**, *16*, 379-389.

(27) Litowski, J. R.; Hodges, R. S. *Journal of Biological Chemistry* **2002**, *277*, 37272.

(28) Moll, J. R.; Ruvinov, S. B.; Pastan, I.; Vinson, C. *Protein Science* **2001**, *10*, 649.

(29) Wagschal, K.; Tripet, B.; Hodges, R. S. *Journal of Molecular Biology* **1999**, *285*, 785.

(30) Yu, Y. B. *Advanced Drug Delivery Reviews* **2002**, *54*, 1113.

(31) Huglin, M. B. *Light scattering from polymer solutions*; Academic Press: London, New York, 1972.

(32) Hellman, U.; Wernstedt, C.; Gonez, J.; Heldin, C. H. *Analytical Biochemistry* **1995**, *224*, 451.